INESEC
INTERNATIONAL ENGINEERING AND NATURAL SCIENCES CONFERENCE (IENSC) 2018

PROCEEDING BOOK

14-17 NOVEMBER 2018
DİYARBAKIR

www. ineseg.org
www.inesegconferences.org

SULFONIC ACID FUNCTIONALIZED NANOCRYSTALLINE MIL-101 METAL ORGANIC FRAMEWORK STABILIZED Ag(0) NANOPARTICLES; SYNTHESIS, CHARACTERIZATION AND ANTIBACTERIAL PROPERTIES

Mehmet Zahmakiran*[1], Sadin Özdemir[2], Serkan Yalçın[3], Gulsah Saydan Kanberoglu[1]

[1]Nanomaterials and Catalysis Research Group, Department of Chemistry, Van Yuzuncu Yil University, zmehmet@yyu.edu.tr , gskanberoglu@yyu.edu.tr

[2]Vocational School of Technical Sciences, Food Technology, Mersin University, sadinozdemir@mersin.edu.tr

[3] Department of Chemical and Chemical Processing Technologies, Technical Science Vocational School, Mersin University, serkanyalcin@mersin.edu.tr

* zmehmet@yyu.edu.tr

Silver(0) nanoparticles stabilized by sulfonic acid functionalized nanocrystalline metal-organic framework (Ag@S-nano-MIL-101) were prepared, for the first time, by using a direct cationic exchange approach and subsequent reduction with sodium borohydride at room temperature. The characterization of the resulting Ag@S-nano-MIL-101 material was done by using multi-pronged analyses, which revealed that the formation of silver(0) nanoparticles (2.95 ± 0.9 nm) stabilized by the framework of nano-S-MIL-101by keeping the host framework intact. The antibacterial properties of the resulting material was investigated against to gram-positive Enterococcus hirae (ATCC 10541) ve Pseudomonas aeruginosa (ATCC 9027) ve Escherichia coli (ATCC 10536) gram-negative bacteria.
Keywords*: Silver nanoparticles, metal-organic framework, nanocrystalline, antibacterial.*

1. Introduction

In recent years, metal nanoparticles have been broadly reconnoitered in the exploration of advanced materials for numerous applications as compared to their bulk-counterparts metal nanoparticles have explicit smart properties [1,2]. Due to the high surface energies and large surface areas, metal nanoparticles are considered as thermodynamically unstable against to agglomeration into bulk and thus protecting ligands, polymers or capping agents must be used to stabilize them in their synthesis [3]. Though, the aggregation of nanoparticles ultimately to the bulk metal despite using the best stabilizing agents [4,5] is still the most vital problem that should be solved in their applications. Moreover, it is another critical subject to attain neat active metal surfaces by evading surface contamination from surface protecting groups, which often leads to a decrease in reactivities. In this context, the usage of porous solid matrices as host material for guest metal nanoparticles immobilization permits the generation of specific surfactant-free active sites with the rewards of avoiding particle aggregation [1–5].

In this regard, porous materials like zeolites [6,7], carbonaceous materials [8,9], and minerals [10,11] have been extensively employed for producing metal nanoparticles within their porous matrices [12]. In addition to these porous materials, more recent studies [13-15] have also revealed that metal-organic frameworks (MOFs), which are crystalline hybrid materials that combine metal

ions with rigid organic ligands [16], can also be considered as proper host materials to stabilize ligand-free guest metal nanoparticles. Definitely, MOFs can act as more suitable support material for metal nanoparticles with respect to other porous solids as they tolerate more flexible and systematic adjustment of the pore structure by the appropriate assortment of the structural subunits and their connected ways [13-16]. Moreover, the stabilization of metal nanoparticles within the structure of MOFs can help us in the kinetic controlling of the process. The accurate selecting of MOF's type under experimental environments is the most precarious step for the employment of MOFs as supports for metal nanoparticle immobilization as only a few MOFs with appropriate pore structures are currently identified for their thermal/chemical stability.

The results of the recent studies are screening that chromium(III) terephthalate framework; MIL-101 ($[Cr_3F(H_2O)_2O\{O_2CC_6H_4(CO_2)\}_3 \cdot nH_2O]$; MIL: Materials Institut Lavosier), which was first reported in 2005 by Ferey et al. [17], can be used in the stabilization of metal nanoparticles as it is stable in water even under very acidic conditions and can show thermal stability up to 300 °C under air [18]. MIL-101 has very high surface area (~4100 m^2/g) and contains two types of cages with diameters of 29 and 34 Å, which have pore apertures of 12 and16 Å, respectively. These unique features of MIL-101 encouraged us to focus on the use of the MIL-101 matrix in the stabilization of metal nanoparticles. Our previous studies have already shown that MIL-101 is suitable support material for the fabrication of active Ru [19] and Rh [20] nanoparticles for the selective hydrogenation of phenol to cyclohexanone. In this study we decided to use nanocrystalline MIL-101 as host material to guest silver nanoparticles. The reduction of the MIL-101 matrix particle size from the microcrystalline to the nanocrystalline regime (from>1 μm to<100 nm) was performed in anticipation of improved activity due to lower mass transfer limitations for antibacterial applications.

2. Experimental

2.1. Materials

Chromium(III) nitrate nonahydrate ($Cr(NO_3)_3 \cdot 9H_2O$), terephthalic acid ($C_8H_6O_4$), dimethylformamide ($HCON(CH_3)_2$), ethanol (C_2H_5OH), methanol(CH_3OH), acetone (CH_3COCH_3), trifluoromethanesulfonic acid (CF_3SO_3H), sulfuric acid (H_2SO_4), sodium borohydride ($NaBH_4$), rhodium(III) chloride trihydrate ($AgNO_3$), nitromethane(CH_3NO_2). All chemicals were used as received without further purification. Nanocrystalline MIL- 101 was synthesized according to literature procedure [21]. The materials isolated at the end of the synthesis were stored in a Labsconco nitrogen atmosphere glovebox (H_2O < 5 ppm, O_2 < 1 ppm). Deionized water was distilled through the water purification system (Milli-Q Water Purification System). All glassware and Teflon-coated magnetic stirring bars were washed with acetone and copiously rinsed with distilled water before drying in an oven at 150 °C.

2.2. Preparation of Sulfonic Acid Functionalized Nano-MIL-101

Sulfonic acid functionalized nano-MIL-101 was prepared by a post-modification method according to the procedure described in the literature [22]. 0.72 g activated nano-MIL-101 was dispersed in 25.0 mL of nitromethane and then trifluoromethanesulfonic anhydride (1.5 mmol) and concentrated sulfuric acid (1.0 mmol) were added into the suspension. Next, the mixture was

continuously stirred in the water bath at room temperature for 1 h. The product was filtered and the solid was rinsed with deionized water and then with acetone, soaked in ethanol for 24 h at 70 °C, and dried in vacuum oven (10^{-1} Torr) at 150 °C for 6 h.

2.3. Preparation of Sulfonic Acid Functionalized Nano-MIL-101 Stabilized Silver Nanoparticles

The activated nano-S-MIL-101 (200 mg) was treated with NaOH in 10.0 mL H_2O to pH 9 and kept at this pH under vigorous agitation for 5 min. Then, filtered and dried host material was added into a solution of $AgNO_3$ (34 mg ca., 0.2 mmol Ag) and this mixture was then stirred for other 6 h. Ag(I)-exchanged S-nano-MIL-101 was isolated by filtration, washed with excess water and dried in vacuum oven (10^{-1} Torr) at 70 °C for 8 h, and then reduced in 1.0 mL aqueous sodium borohydride (220 mg; $[NaBH_4]/[M] = 30$) kept in ice-bath. Afterwards the solid was centrifuged and washed with deionized water and ethanol and dried in vacuum oven (10^{-1} Torr) at 70 °C for 8 h. The silver content of Ag@S-nano-MIL-101 was found to be 2.05 wt% by ICP-OES.

2.4. Characterization of Ag@S-nano-MIL-101

The amount of silver loaded on S-nano-MIL-101 was determined by inductively couple plasma optical emission spectroscopy (ICP-OES) by using Perkin Elmer DR-CII model (detection limit is 16 ppb for Ag). Elemental analyses were performed on LECO, CHNS-932 model. The powder X-ray diffraction (P-XRD) analyses were carried out on Rigaku Ultima-IV by using Cu-Kα radiation (wavelength 1.54 Å, 40 kV, 55 mA). BFTEM samples were prepared by dropping one drop of dilute suspension on copper coated carbon TEM grid and the solvent was then dried. BFTEM was carried out on a JEOL JEM-200CX transmission electron microscopes operating at 120 kV. The XPS analyses were performed on a Physical Electronics 5800 spectrometer equipped with a hemispherical analyzer and using monochromatic Al-Kα radiation (1486.6 eV, the X-ray tube working at 15 kV and 350 W, and pass energy of 23.5 eV). DR-UV–vis analyses were performed on Shimadzu UV-3600 modulated with integrating sphere attachment.

2.5. Antibacterial Activity Studies

Gram-positive bacteria of *Entorococcus hirae* (ATCC 10541) and Gram-negative bacteria of *Pseudomonas aeruginosa* (ATCC 9027) and *E. coli* (ATCC 10536) were used to display the antibacterial activity of Ag(0) nanoparticles. Prior to antibacterial studies, culture medium and all glassware were autoclaved for 20 min at 121 °C. The minimal inhibition concentration (MIC) were evaluated by two-fold serial broth dilution process to define the antibacterial abilities of the newly synthesized Ag(0) nanoparticles. MIC is described as the lowest concentration of the studied samples at which the visible growth of the bacteria, defined by turbid-metric process after incubation, is inhibited. The serial broth mediums containing various concentrations (5000, 2500, 1250, 625, 312.5, 156.25, 78.125, and 0 mg/mL) of Ag(0) nanoparticles were separately mixed with bacterial culture containing 10^8-10^9 colony-forming units (CFU)/mL. The culture mediums were incubated at 37 °C and 120 rpm for 24 h in a shaker.

3. Results and Discussion

To begin with, as-prepared Ag@S-nano-MIL-101 was characterized by multi-pronged analyses including ICP-OES, EA, P-XRD, XPS, DR-UV–vis, SEM, BFTEM and N_2-adsorption–desorption techniques. The EA and ICP-OES analyses revealed that the existence of S (0.27 wt%; 0.89 mmol/g; S/Cr = 0.87) and Ag (2.05 wt%; 0.21 mmol/g; S/Ag = 4.23) in the synthesized Ag@S-nano-MIL-101. The crystallinity of the host nano-MIL-101 framework throughout the formation of both S-nano-MIL-101 and Ag@S-nano-MIL-101 was investigated by P-XRD (Figure 1). The wide angle P-XRD patterns of S-nano-MIL-101 and Ag@S-nano-MIL-101 showed the characteristic reflections of the host matrix S-nano-MIL-101 [17], which confirmed the intact structure of nano-MIL-101 after sulfonic acid functionalization and silver(0) nanoparticles formation.

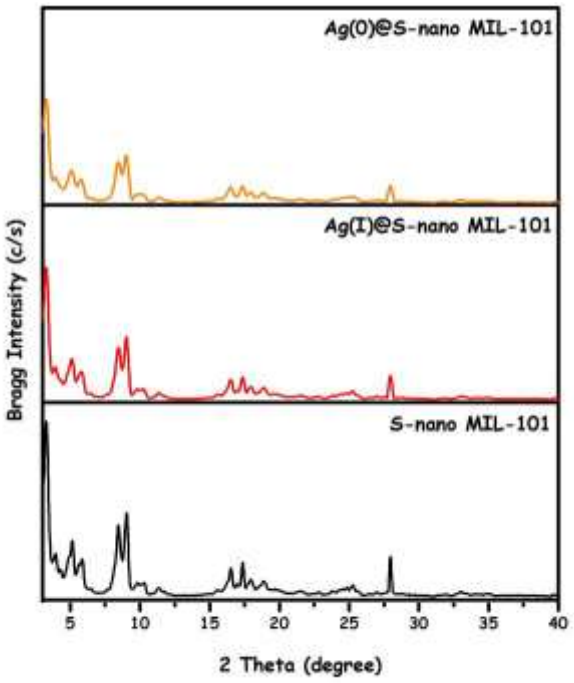

Figure 1. P-XRD patterns of S-nano-MIL-101, Ag(I)@S-nano-MIL-101 and Ag(0)@S-nano-MIL-101 samples in the range of 2θ = 3-40°.

The decrease of the overall Bragg peaks intensity with respect to the parent host material MIL-101 was a consequence of the inclusion of guest particles within the framework and has been well studied for zeolites and mesoporous silica materials [23, 24]. In summary, the sum of P-XRD results is showing that neither the crystallinity nor the lattice of MIL-101 is distorted by formation of Ag nanoparticles within the sulfonic acid functionalized framework of nano-S-MIL-101. Figure 2 shows DR-UV–vis spectra of nano-MIL-101, S-nano-MIL-101 and Ag@S-nano-MIL-101. The absorption bands observed at 450 and 602 nm in all of three nano-MIL-101, S-nano-MIL-101 and Ag@S-nano-MIL-101 samples indicate that Cr(III) is present in distorted octahedral form [25]. After the sulfonic acid functionalization and silver incorporation, there was no distinguishable change observed in the DR-UV–vis bands, which is also revealing of host framework was kept at the end of the synthesis of both, S-nano-MIL-101 and Ag@S-nano-MIL-101.

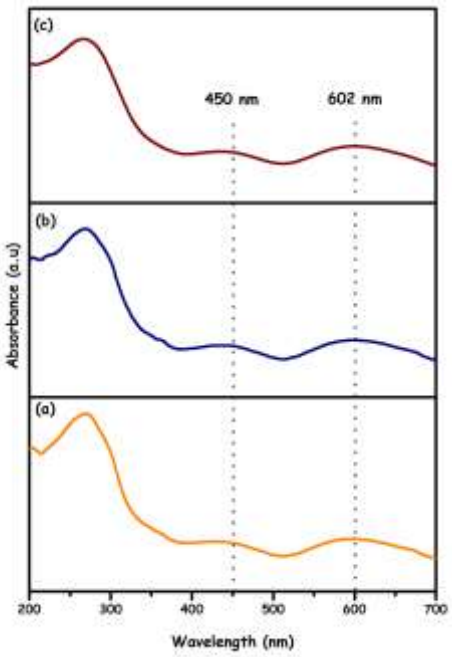

Figure 2. DR-UV–vis spectra of (a) nano-MIL-101, (b) S-nano-MIL-101 and (c) Ag@S-nano-MIL-101 (2.05 wt % Ag) in the range of 200–700 nm.

The FTIR spectra of the synthesized nano-MIL-101 and Ag@S-nano-MIL-101 samples are given together in Figure 3. Apart from nano-MIL-101, for Ag@S-nano-MIL-101 new bands appeared at 1280, 1190, 1080, 1040 and 665 cm^{-1}. The bands observed at 1280 and 1190 cm^{-1} can be ascribed to O=S=O symmetric and asymmetric stretching modes [26] and the peak at 1080 cm^{-1} is resulting from the S-O stretching vibration [26,27]. The peak at 665 cm^{-1} may be assigned to C-S stretching vibration [28] and the additional peak at 1080 cm^{-1} corresponds to the skeletal vibration of the benzene rings substituted by a sulfonic acid group [26,27].

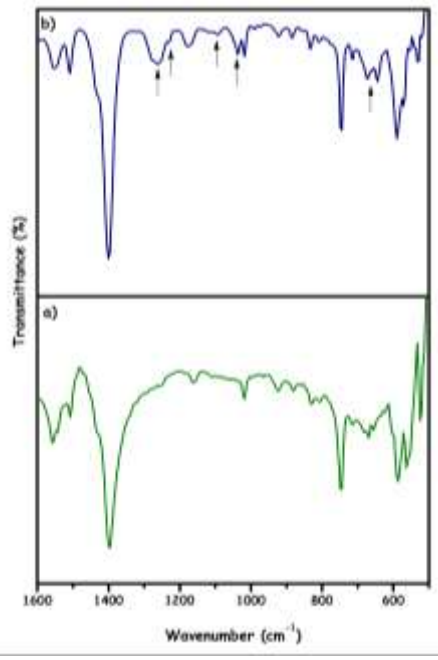

Figure 3. FTIR spectra of (a) nano-MIL-101, (b) Ag@S-nano-MIL-101 (2.05 wt% Ag) in the range of 1600-600 cm^{-1}

Then, XPS spectrum of Ag@S-nano-MIL-101 was taken in the range of BE= 360-385 eV for Ag 3d core level (Fig. 4). As shown in Fig. 4 this spectrum shows two distinct bands around 366 and 372 eV which can be assigned to metallic silver Ag(0) [9].

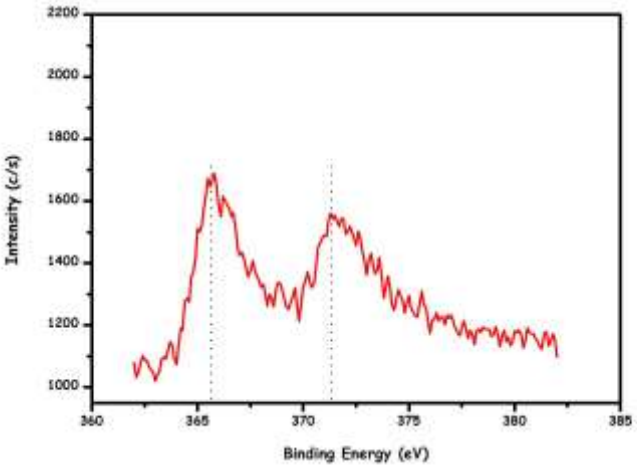

Figure 4. XPS spectrum of Ag@S-nano-MIL-101 (2.05 wt% Ag) in the range of BE= 360-385 eV.

The morphological investigation of Ag@S-nano-MIL-101 was done by SEM and BFTEM analyses. SEM images of Ag@S-nano-MIL-101 at different magnifications were given in Figure 5, these SEM images show only crystalline nano-MIL-101 framework and there is no bulk Ag accumulation is observed in these images.

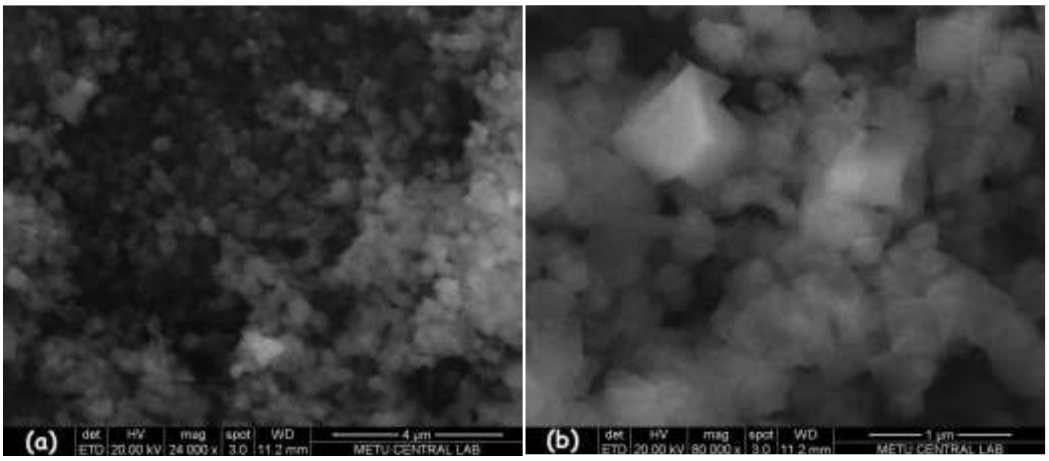

Figure 5. (a) and (b) SEM images of Ag@S-nano-MIL-101 (2.05 wt% Ag) in different magnifications.

BFTEM images of Ag@S-nano-MIL-101 shows the existence of well-dispersed Ag nanoparticles on the framework of nano-MIL-101 (*Figure 6*). The mean particle size of these particles was found to be 2.95 ± 0.9 nm (Figure 6). Additionally, STEM-EDX spectrum collected throughout the BFTEM observations shows that the existence of silver in the analyzed regions (Figure 7).

The antibacterial properties of the resulting material was investigated against to gram-positive Enterococcus hirae (ATCC 10541), Pseudomonas aeruginosa (ATCC 9027) and Escherichia coli (ATCC 10536) gram-negative bacteria. In all samples (containing different amount of silver) Ag@S-nano-MIL-101 shows antibacterial activity (Figure 8).

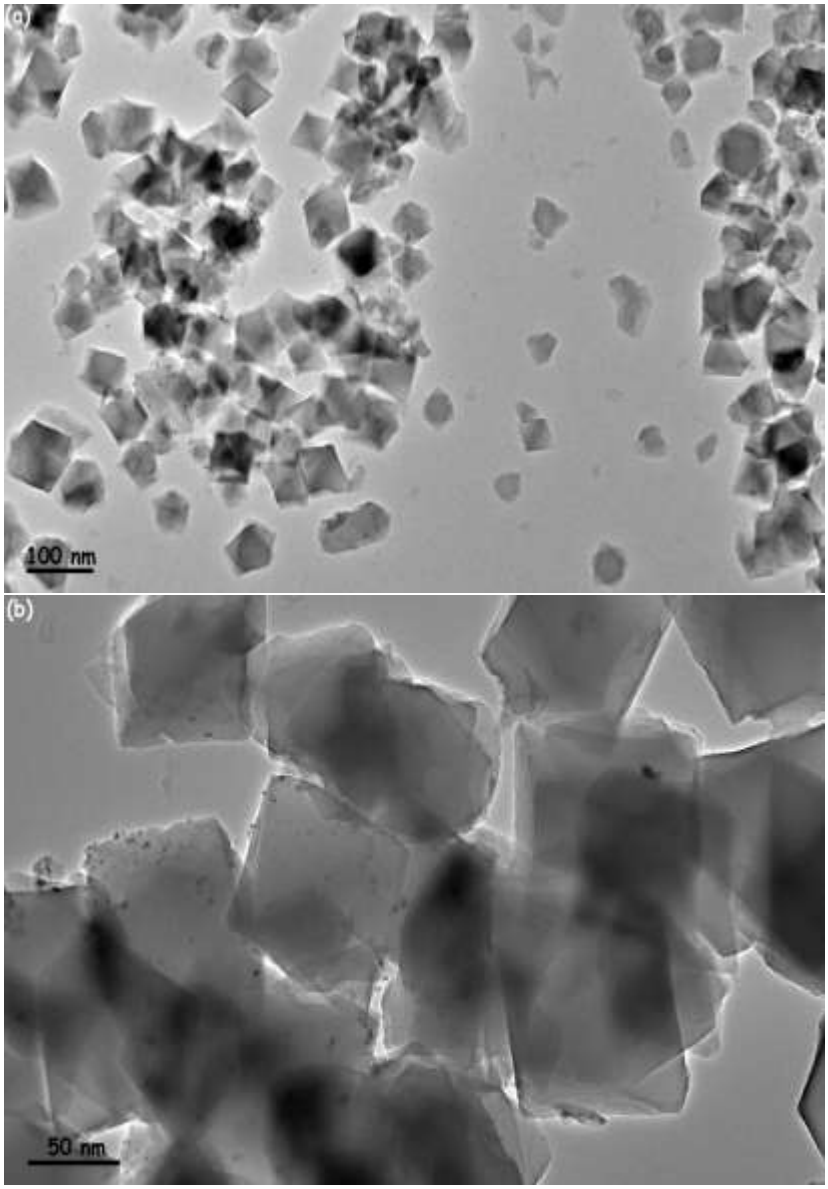

Figure 6. (a)-(b) BFTEM images of Ag@S-nano-MIL-101 (2.05 wt% Ag) in different magnifications.

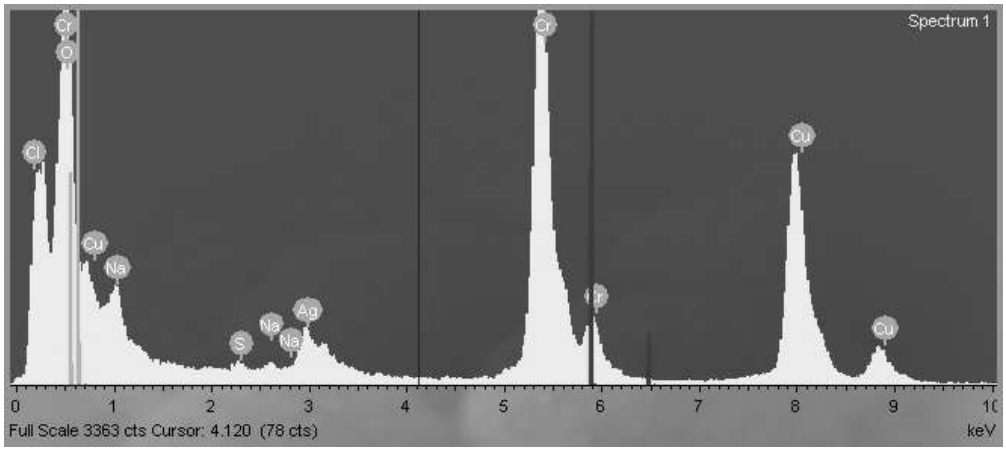

Figure 7. STEM-EDX spectrum of Ag@S-nano-MIL-101 (2.05 wt% Ag).

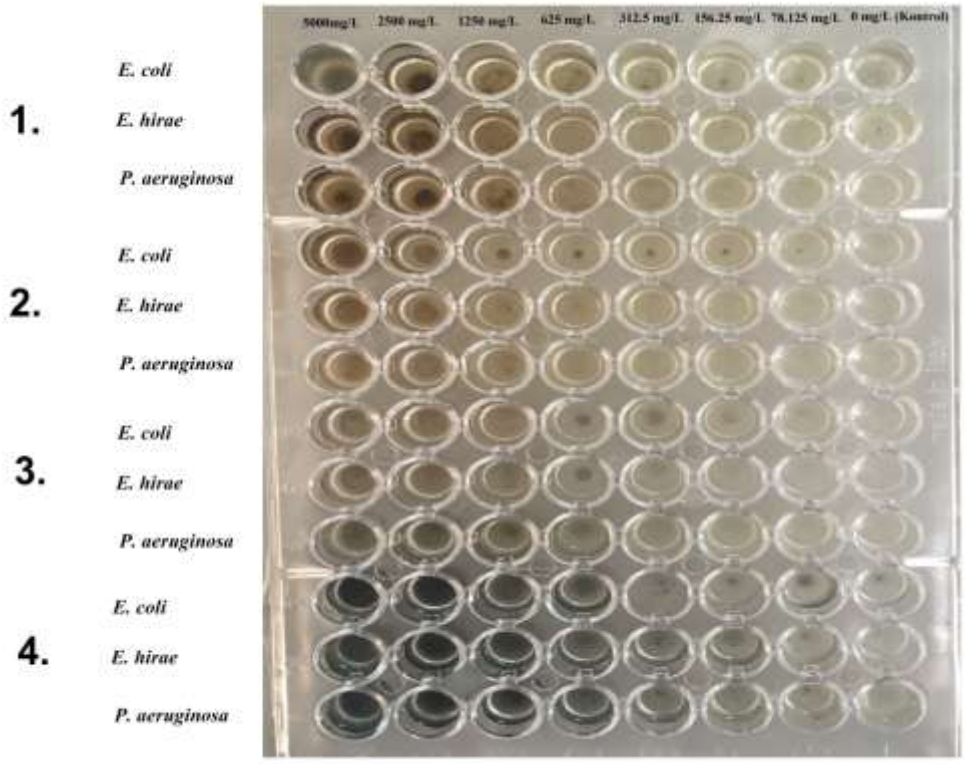

Figure 8. Antibacterial activity results of Ag@S-nano-MIL-101 (2.05 wt% Ag) against to gram-positive Enterococcus hirae (ATCC 10541), Pseudomonas aeruginosa (ATCC 9027) and Escherichia coli (ATCC 10536) gram-negative bacteria.

Acknowledgment

The financial support by the Scientific and Technological Research Council of Turkey (TUBITAK, Project No: 116Z555) is gratefully acknowledged.

References

[1] M. Zahmakiran, S. Ozkar, *Nanoscale* 3 (2011) 3462.

[2] D. Astruc, F. Lu, J.R. Aranzaes, *Angew. Chem. Int. Ed.* 44 (2005) 7852.

[3] B. L. Cushing, L. Kolesnichenko, C.J. Connor, *Chem. Rev*. 104 (2004) 3893.

[4] S. Özkar, R.G. Finke, *J. Am. Chem. Soc*. 124 (2002) 5796.

[5] S. Özkar, R.G. Finke, *Langmuir* 19 (2003) 6247.

[6] M. Zahmakiran, S. Özkar, *Langmuir* 24 (2008) 7065.

[7] L. Tosheva, V. P. Valtchev, *Chem. Mater*. 17 (2005) 2494.

[8] E. Castillejos, P. J. Debouttire, L. Roiban, A. Solhy, V. Martinez, Y. Kihn, O. Ersen, K. Philippot, B. Chaudret, P. Serp, *Angew. Chem. Int. Ed.* 48 (2009) 2529.

[9] M. Yurderi, A. Bulut, M. Zahmakiran, M. Kaya, *Appl. Catal. B Environ*. 160 (2014) 514.

[10] M. Zahmakiran, Y. Tonbul, S. Özkar, *Chem. Commun.* 46 (2010) 4788.

[11] M. Zahmakiran, Y. Roman-Leshkov, Y. Zhang, *Langmuir* 28 (2012) 60.

[12] R.J. White, R. Luque, V.L. Budain, J.H. Clark, D.J. Macquarrie, *Chem. Soc. Rev*. 38(2009) 481.

[13] J.Y. Lee, O.K. Farha, J. Roberts, K.A. Scheidt, S.T. Nguyen, J.T. Hupp, *Chem. Soc. Rev*. 38 (2009) 1450.

[14] A. Corma, H. Garcia, F.X.L. Xamena, *Chem. Rev*. 110 (2010) 4606.

[15] A. Aijaz, Q. Xu, *J. Phys. Chem. Lett.* 5 (2014) 1400.

[16] J. L. C. Rowsell, O. M. Yaghi, *Mic. Mes. Mater*. 73 (2004) 3.

[17] G. Ferey, C.M. Draznieks, C. Serre, F. Millange, J. Dutour, S. Surble, I. Margiloski, *Science* 309 (2005) 2040.

[18] A. Khutia, H.U. Remmelberg, T. Schmidt, S. Henninger, C. Janiak, *Chem. Mater*. 25 (2013) 790.

[19] I.E. Ertas, M. Gulcan, M. Yurderi, A. Bulut, M. Zahmakiran, *J. Mol. Catal. A: Chem.* 410 (2015) 209–220.

[20] I.E. Ertas, M. Gulcan, M. Yurderi, A. Bulut, M. Zahmakiran, *Mic. Mes. Mater*. 226 (2016) 94–103.

[21] D. Jiang, A. D. Burrows, K. J. Edler, *CrysEngComm* 13 (2011) 6916–6919.

[22] M.G. Goesten, J. J. Alcaniz, E.V. Ramos-Fernandez, K. Gupta, E. Stabitski, H. VanBekum, J. Gascon, F. Kapteijn, *J. Catal*. 281 (2011) 177.

[23] M. Zahmakiran, S. Özkar, *Mater. Lett*. 63 (2009) 1033.

[24] M. Zahmakiran, S. Özkar, *J. Mater. Chem*. 19 (2009) 7112.

[25] M. Annapurna, T. Parasuramulu, P. Vishnuvardhan, M. Suresh, P. R. Likhar, M. L.Kantam, *Appl. Org. Chem*. 29 (2015) 234.

[26] Y. Zhang, J. Shi, F. Zhang, Y. Zhong, W. Zhu, *Catal. Sci. Technol*. 3 (2013) 2044.

[27] B. Ostrowskagumkowska, J. Ostrowskaczubenko, *Eur. J. Polym*. 30 (1994) 869.

[28] H. Liu, T. Jiang, B. Han, S. Liang, Y. Zhou, *Science* 326 (2009) 1250.